Olefin Metathesis in Confinement: Towards Covalent Organic Framework Scaffolds for Increased Macrocyclization Selectivity

Sebastian T. Emmerling,[a][b]‡ Felix Ziegler,[c]‡ Felix R. Fischer,[d] Roland Schoch,[e] Matthias Bauer,[e] Bernd Plietker,[d] Michael R. Buchmeiser,[c] and Bettina V. Lotsch*[a][b][f]

[a]   S.T. Emmerling, Prof. B.V. Lotsch
        Nanochemistry Department
        Max Planck Institute for Solid State Research
        Heisenbergstraße 1, 70569 Stuttgart, Germany
        E-mail: b.lotsch@fkf.mpg.de
[b]   S.T. Emmerling, Prof. B.V. Lotsch
        Department of Chemistry
        University of Munich (LMU)
        Butenandtstraße 5–13, 81377 Munich, Germany
[c]   F. Ziegler, Prof. M.R. Buchmeiser
        Institute of Polymer Chemistry
        University of Stuttgart
        Pfaffenwaldring 55, D-70569 Stuttgart, Germany
[d]   F. Fischer, Prof. B. Plietker
        Faculty of Chemistry and Food Chemistry
        Technical University of Dresden
        Bergstrasse 66, D-01069 Dresden, Germany
[e]   Dr. Roland Schoch, Prof. M. Bauer
        Department of Chemistry
        Paderborn University
        Faculty of Science and Center for Sustainable Systems Design (CSSD)
        Warburger Str. 100, D-33098 Paderborn, Germany
[f]   Prof. B.V. Lotsch
        E-conversion and Center for Nanoscience
        Lichtenbergstraße 4a, 85748 Garching, Germany
‡   Authors contributed equally

        Supporting information for this article is given via a link at the end of the document.

Abstract: Covalent organic frameworks (COFs) offer vast structural and chemical diversity enabling a wide and growing range of applications. While COFs are well-established as homogeneous catalysts, so far, their high and ordered porosity has scarcely been utilized to its full potential when it comes to spatially confined reactions in COF pores to alter the outcome of reactions. Here, we present a highly porous and crystalline, large-pore COF as catalytic support in α,ω-diene ring-closing metathesis reactions, leading to increased macrocylization selectivity. COF pore-wall modification by immobilization of a Grubbs-Hoveyda-type catalyst via a mild silylation reaction provides a molecularly precise heterogeneous metathesis catalyst. An increased macro(mono)cyclization (MMC) selectivity over oligomerization (O) for the heterogeneous COF-catalyst (MMC:O = 1.30) of up to 44% compared to the homogeneous catalyst (MMC:O = 0.90) was observed along with a substrate-size dependency in selectivity, pointing to diffusion limitations induced by the pore confinement.

Introduction

Covalent organic frameworks (COFs) are 2D or 3D polymers, which are defined by their covalent connectivity, porosity, and crystallinity, while consisting exclusively of light elements.[1] The vast structural and chemical diversity of COFs and the possibility to tune their framework with atomic precision has put COFs in the spotlight for a variety of applications that benefit from precise framework design, including photocatalytic water splitting,[2,3] sensing,[4] batteries,[5] gas adsorption,[6] or heterogeneous catalysis.[7] With their ordered micro- and mesoporosity and large
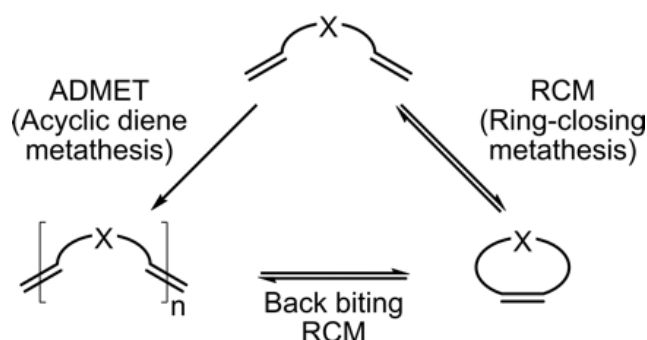
Scheme 1. Competing metathesis reactions of α,ω-dienes resulting in macro(mono)cycles and oligomerization products.

specific surface areas exposing a large number of functional or even active catalytic sites, COFs are among the most promising materials for molecular heterogeneous catalysis. Classical approaches to design COFs for heterogeneous catalysis utilizing this feature include incorporation of catalytic centers directly in the pore wall,[8] pore surface engineering by molecular catalysts *via* a post-synthetic reaction,[9] integration of monodisperse nanoparticles in the framework by pore templating, or embedding polymers into the pores to combine multiple catalytic centers.[10,11] However, despite the promise of COFs as versatile scaffolds for catalysis, examples for the exploitation of reaction-specific pore confinement effects during catalysis, such as the substrate-specific and size-selective Knoevenagel-reaction achieved for microporous COFs by Fang *et al.*,[12] are still rare. Altering selectivity and reactivity of the catalyzed reaction by spatial confinement is an immensely successful principle used in nature
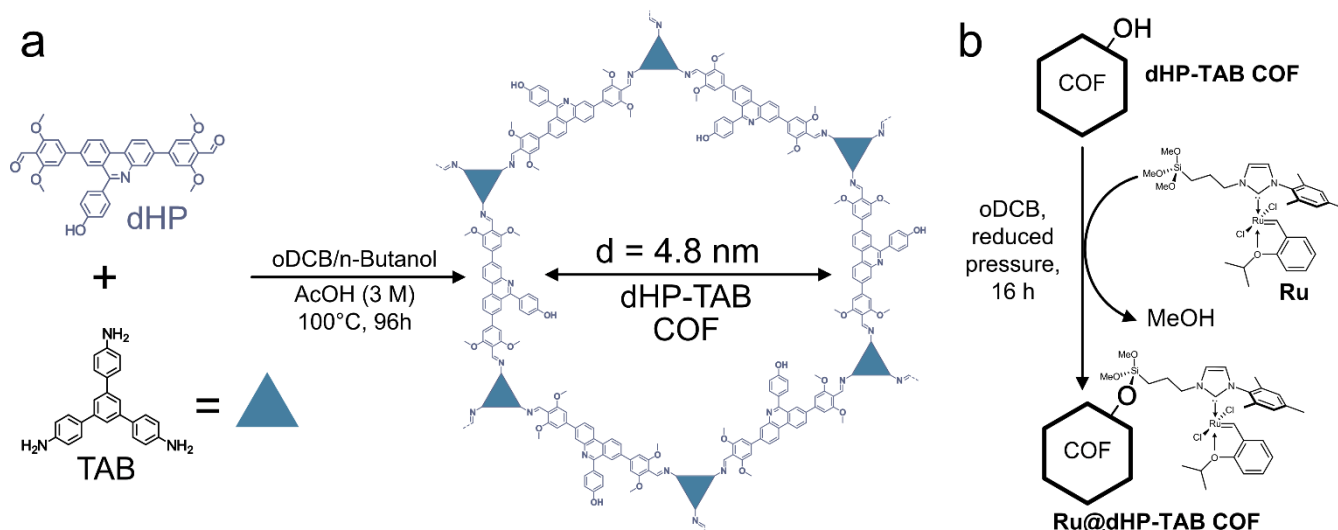
1

Figure 2. (a) Synthesis of **dHP-TAB** COF. (b) Immobilization of **Ru** catalyst on **dHP-TAB** by silylation to form **Ru@dHP-TAB**.

by enzymes and enzyme-inspired artificial catalysis. Taking full advantage of the ordered structural porosity of COFs thus bodes well for a biomimetic approach to catalysis where the precise spatial arrangement of catalytic centers and substrates, as well as pore confinement is utilized to direct product selectivity.[13]

In this work, we present a large-pore imine-COF as a molecular heterogeneous catalyst to study the effect of spatial confinement on product selectivity during olefin metathesis reactions; in particular macro(mono)cyclization (MMC) selectivity by ring-closing metathesis (RCM) and back-biting depolymerization vs. acyclic diene metathesis (ADMET) oligomerization (O, Scheme 1).

Olefin metathesis-based macrocyclization offers an important pathway to useful compounds for industrial or pharmaceutical chemistry,[14] however, still poses severe challenges. Oftentimes, only low MMC yields are achieved due to the competing oligomerization by ADMET, originating from a ring-chain equilibrium during catalysis and back-biting RCM.[15,16] The biomimetic approach by spatial confinement of metathesis reactions in pores for increased selectivity towards MMC products was already successfully shown for mesoporous silica by Jee *et al.* and Ziegler *et al.*[16,17] Applying this biomimetic approach to a COFs system not only diversifies the scope of possible confinement effects and framework-catalyst-reactant interactions, but at the same time offers new opportunities for precise, substrate- and product-specific catalyst-framework designs due the high structural and chemical diversity of COFs.

Results and Discussion

For the study of olefin metathesis reactions under spatial confinement in COFs, the model system, **dHP-TAB** COF, was synthesized by the condensation of 4,4'-(6-(4-hydroxyphenyl)phenanthridine-3,8-diyl)bis(2,6-dimethoxybenzaldehyde) (**dHP**) and 5'-(4-aminophenyl)-[1,1':3',1''-terphenyl]-4,4''-diamine (**TAB**) in a solvent mixture of 1,2-dichlorbenzene (oDCB) and *n*-butanol (3 : 7) with 3 M acetic acid (AcOH) as catalyst for 96 h at 100°C. After isolation by filtration, the solid was washed and subsequently activated by supercritical CO_2 (Figure 1, a). The large-pore COF system was chosen to accommodate the bulky catalyst and substrates and prevent pore blocking during immobilization and catalysis. Methoxy groups incorporated in the COF act as non-covalent
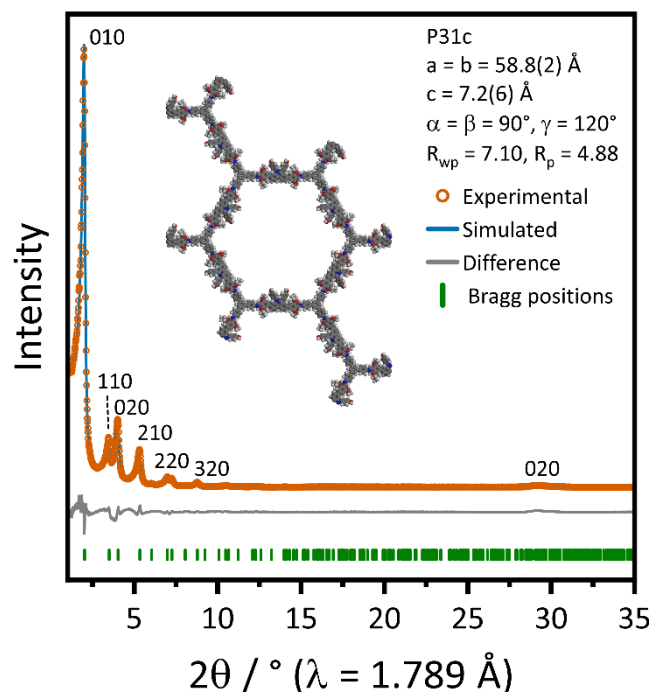

Figure 1. Experimental XRPD pattern of **dHP-TAB** COF, Rietveld fit, difference curve and positions of the Bragg reflections. Inset: Structure of the respective AĀ-stacked **dHP-TAB** along the *a* and *b* axis after refinement.

anchors to achieve better layer registry and thus high porosity and large, well-defined pore sizes for this framework.[18]

Imine formation during the initial COF synthesis was confirmed by FT-IR analysis (Figure S7). The spectrum shows the absence of the prominent aldehyde C=O stretching band at 1674 cm^{-1} and amine N-H stretching bands at 3355 cm^{-1} and 3431 cm^{-1}, corresponding to the starting materials, indicating full conversion into imine bonds. The new imine stretching band is mostly concealed as slight shoulder at around 1614 cm^{-1} of the strong aromatic C-C stretching bands at 1593 cm^{-1}. The solid-state [13]C
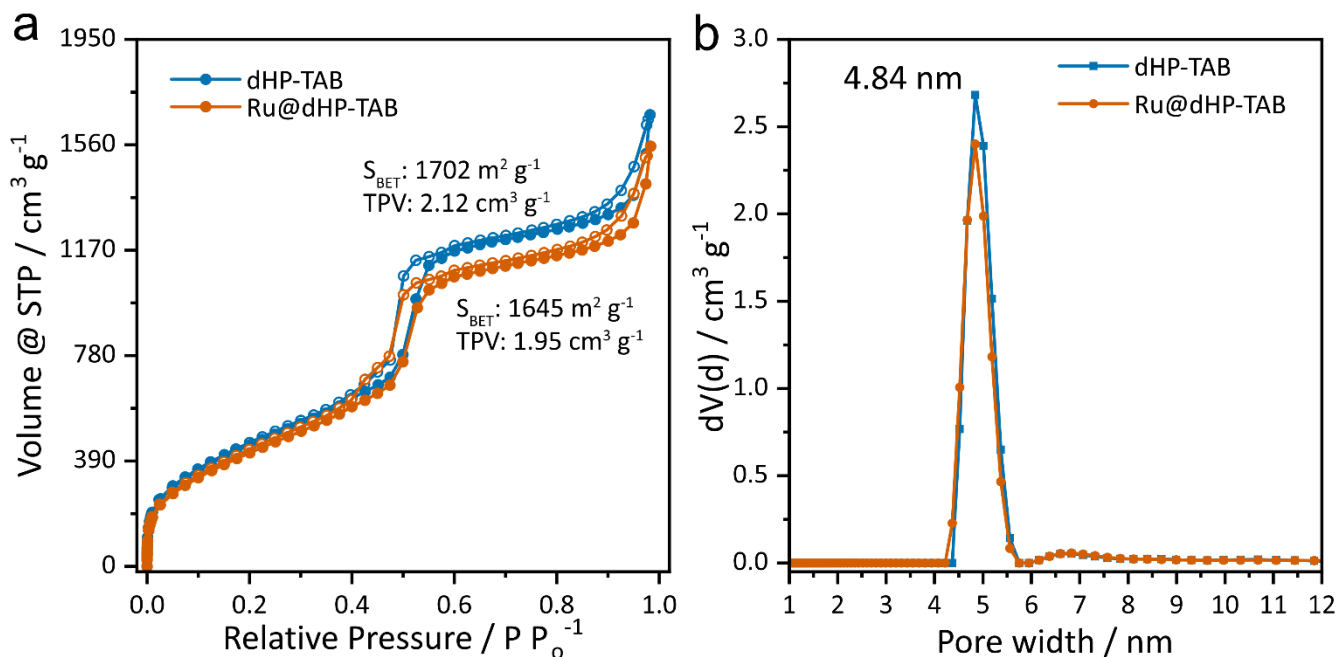
Figure 3. Comparison of (a) nitrogen isotherms at 77 K (filled circles for adsorption, empty circles for desorption) and (b) pore size distribution obtained from the adsorption branch of **dHP-TAB** and **Ru@dHP-TAB** after immobilization of the catalyst.

resonance (CP-MAS ssNMR) spectrum confirms the successful condensation by showing the typical imine signal at 160.0 ppm and the absence of aldehyde signals (Figure S12).

Crystallinity of **dHP-TAB** COF was confirmed by X-ray powder diffraction (XRPD), with the pattern (Co-K$_{\alpha 1}$) displaying several well-resolved diffraction peaks at 2 θ = 2.01°, 3.49°, 4.02°, 5.32°, 6.97°, 7.25°, 8.78°, 10.47° and a broadened stacking reflection centered around 28.52° (Figure 2).

The structure was modeled in P31c symmetry with an alternating nearly-eclipsed A$\overline{\text{A}}$ stacking order of the layers. This assumed model is based on previous findings for phenylphenanthridine based COFs[18] and shows a good match when compared to the simulated patterns of an A$\overline{\text{A}}$ stacked model (Figure S10). Rietveld refinement of the pattern with the assumed model yielded unit cell parameters ($a = b$ = 58.8(2) Å and c = 7.2(6) Å) with a statisfying agreement factor (R$_{wp}$ = 7.10%, R$_p$ = 4.88%) (Figure 2).

Porosity of **dHP-TAB** COF was investigated by nitrogen physisorption measurements at 77 K, showing a type-IV isotherm, which is typical for mesoporous systems. The Brunauer-Emmett-Teller surface area (S$_{BET}$) was calculated to be 1702 m^2 g^{-1} with a total pore volume of 2.12 cm^3 g^{-1} at P/P$_0$ = 0.95. The pore size distribution (PSD) was determined from the adsorption branch by quenched solid density functional theory (QSDFT) based on the carbon model for cylindrical pores. It shows a narrow PSD around 4.8 nm, which is in good agreement with the structure model and closely related, isoreticular COFs.[18]

Next, the molecular catalyst RuCl$_2$(N-mesityl-N-(3-(trimethoxysilyl)prop-1-yl)-imidazol-2-ylidene)(CH-2-(2-PrO-C$_6$H$_4$)) (**Ru**) was immobilized in the framework *via* silylation, utilizing the incorporated hydroxyl groups of the protruding phenols as anchor points (Figure 1, b). The immobilization was performed at room temperature in high-boiling oDCB as solvent under reduced pressure. Performing the reaction under vacuum significantly increases the catalyst loading by removing the accruing methanol from the reaction mixture and driving the reaction towards the desired outcome, yielding the catalyst-loaded **Ru@dHP-TAB** COF. Inductively-Coupled Plasma Optical Emission Spectroscopy (ICP-OES) of the washed and dried sample revealed a Ru-content of c(Ru) = 42.3 µmol/g for **Ru@dHP-TAB** COF. This corresponds to a successful silylation of approximately 3.4 % of the hydroxyl groups contained in the COF.

No changes in the FT-IR spectra of **Ru@dHP-TAB** compared to the pristine COF are visible, which can be attributed to the comparatively low amounts of immobilized catalyst (Figure S8) and the XRPD pattern shows a retention of COF crystallinity (Figure S9). Nitrogen sorption measurements reveals only a minimal reduction in surface area (S$_{BET}$ = 1645 m^2 g^{-1}) und total pore volume (1.95 cm^3 g^{-1} at P/P$_0$ = 0.95) compared to **dHP-TAB** with nearly identical pore size distribution (Figure 3). The largely retained porosity suggests that no substantial fraction of pores was fully blocked during the immobilization.

To confirm the stability of the catalyst during immobilization and to gain knowledge of the catalyst's structure in the pore, X-ray absorption (XAS) measurements were performed. Spectra of **Ru** and **Ru@dHP-TAB** as solids and in solution/suspension (benzene), respectively, were recorded,

The obtained X-ray absorption near edge structure (XANES) spectra (Figure 4, a and Figure S14), providing information about the oxidation state of the Ru-metal center,[19] shows no differences in the edge energy for all four samples measured. A change in the electronic structure or oxidation state by immobilization in the COF can thus be excluded

Results of extended X-ray absorption fine structure (EXAFS) analysis, probing the local geometric structure around an X-ray absorbing atom of the **Ru** catalyst under homogeneous and immobilized conditions are shown in Figure 4, b.[20] The corresponding first shell scattering paths combined with coordination numbers, bond distances and Debye-Waller factors, which describe the static and dynamic disorder in the coordination shell, are collected in Figure S16 and Table S7. The results of the structure analysis for all samples are in good
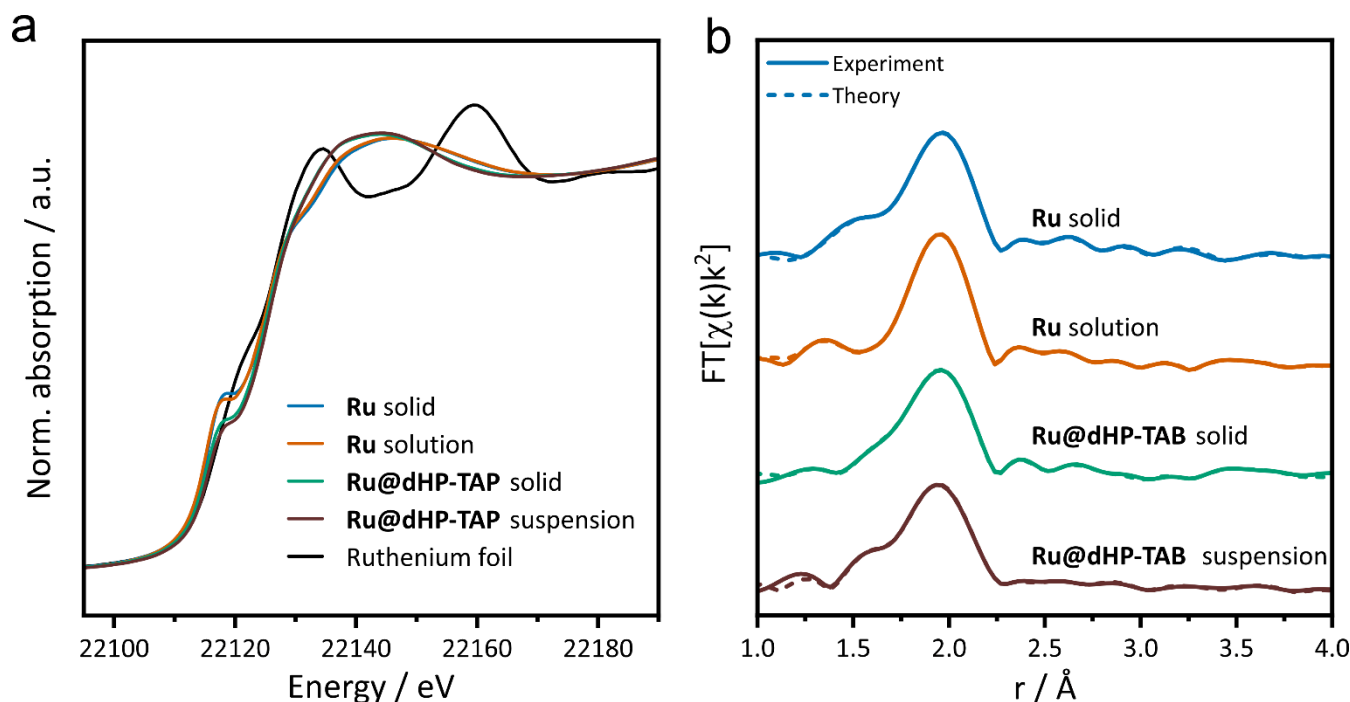
Figure 4. (a) XANES spectra of the homogeneous **Ru** complex in the solid state (red), solution (green), immobilized in the mesoporous COF in the solid state (yellow), as suspension in benzene (brown), as well as of the Ru(0) foil used for calibration (black). (b) Fourier-transformed EXAFS data of the four Ru complexes. Continuous line: experimental data, dotted line: fitted data.

agreement with the single-crystal structure of the **Ru** catalyst.[16] In the solid immobilized sample **Ru@dHP-TAB**, the second Ru-C distance is sligthy elongated compared to the pure **Ru** complex, and the coordination number of this shell is increased. Since the changes cannot be explained by major structural modifications, they are assigned to the effect of the immobilization, such as pore wall interactions. This conclusion is backed by the results for **Ru@dHP-TAB** in benzene, where the structural alterations are reversed, as identified by structural parameters very similar to those of **Ru** in solution. Based on these observations, it can be concluded that neither the dissolution of the homogeneous complex in benzene nor the immobilization in a mesoporous COF lead to significant changes of the complex structure, which stays intact after immobilization. Neither ligand dissociation nor an association can be observed.

After confirmation of the stability of the COF framework and its immobilized catalyst, metathesis reactions were carried out to determine the catalytic efficiency and the effect of the spatial confinement on MMC:O product selectivity. For this purpose metathesis reactions of four substrates (Figure 5, a), differing in their hydrodynamic radius[16] and polarity were performed with the homogeneous **Ru** as well as with **Ru@dHP-TAB.** The reactions were carried out under identical conditions at 50 °C for 16 h in C_6D_6 using 0.5-mol% of catalyst and a substrate concentration of 25 mM; results are summarized in Table 1.

The immobilization significantly alters the productivity of the catalyst, reducing the overall conversion after 16 h reaction time from around 80% to around 10%. This reduction was consistent for all substrates, independent of their size. This drastically reduced productivity is attributed to diffusion limitations and catalyst decomposition occurring during the reaction. However, a size-dependent increase in selectivity MMC:O was found for the catalysis with **Ru@dHP-TAB** compared to **Ru** (Figure 5, b). For the smallest substrate **1** (8.81 Å), an increase of 44% in the MMC:O ratio from 0.90 for **Ru** to 1.30 for **Ru@dHP-TAB** was

found, corresponding to a 9 % increase in selectivity compared to the homogeneous catalyst system. Furthermore, a continuously reduced macromonocyclization selectivity with increasing substrate size is observed. For substrate **4** (9.05 Å), with a very similar radius to **1**, the MMC:O ratio is increased by 33%.

Table 1. Conversion, MMC:O ratio and selectivity for the RCM of substrate **1** - **4** by the action of **Ru** (0.5 mol-%) and **Ru@dHP-TAB** (0.5 mol-%) as determined by NMR (Figure S2-6).

Substrate	Conversion [%]		MMC:O		MMC Selectivity [%]	
	Ru	Ru@ dHP-TAB	Ru	Ru@ dHP-TAB	Ru	Ru@ dHP-TAB
1	81	11	0.90	1.30	47	56
2	77	11	0.84	0.98	46	49
3	80	11	0.65	0.63	39	39
4	73	12	0.40	0.53	28	35

The very similar increase in selectivity for **1** and **4** with almost identical size but different polarity suggests that the polarity of the substrate has little influence on the reaction outcome. For the second largest substrate **2** (10.64 Å) only 17% are achieved and the largest substrate **3** (11.71 Å) shows the same selectivity when catalyzed by **Ru@dHP-TAB** compared to the homogeneous **Ru**. This considerable size effect is rationalized by the substrate diffusion limitation into the COF mesopores pores with increasing hydrodynamic radius. In the case of larger substrates, the reaction is mostly catalyzed by catalyst bound on the outer surface and close to the pore openings, mimicking the homogeneous ring-chain equilibrium.[15] Smaller substrates can diffuse more easily and penetrate into the COF pores more deeply, where pore confinement effects can take place, favoring RCM for the ring-
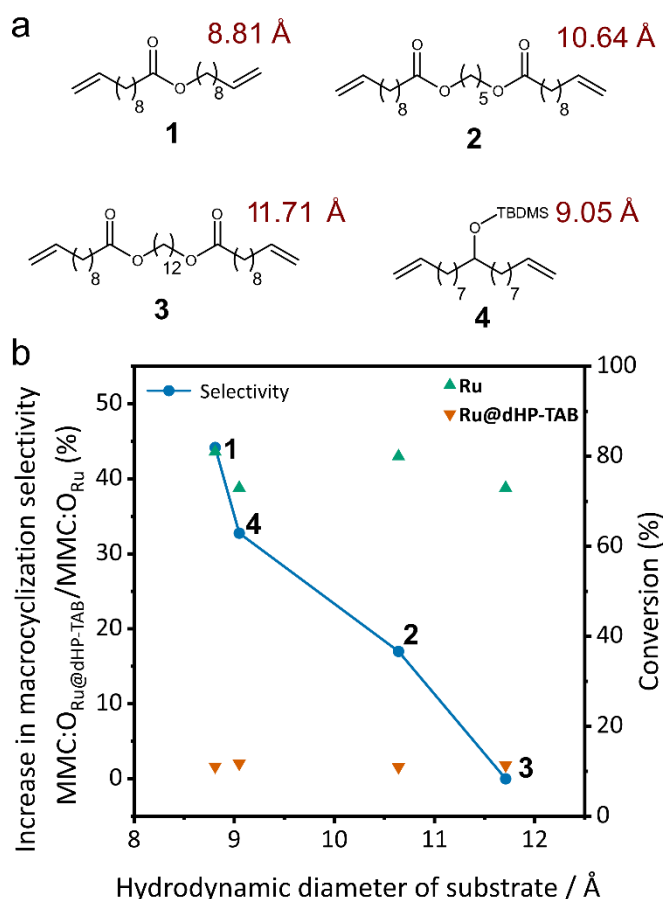
Figure 5. (a) Substrates 1-4 used in this study and their respective hydrodynamic radius (red) acc. to Ziegler *et al.*[16] (b) Correlation between the hydrodynamic radii of the substrates and increase in macrocyclization selectivity (blue) and conversion rate for the homogeneous (green) and heterogeneous catalyst (orange).

chain equilibrium products of the reaction by suppressing the formation of higher oligomers.[21,22]. This is likely due to the very large internal surface area of the highly porous COF material that offers enough "inner" pore surface area for this size selective confinement effect to take place and to alter the ring-chain equilibrium.

Conclusion

In summary, we have developed a phenylphenanthridine-based COF, containing accessible hydroxyl-groups on its protruding phenyl groups that allowed the successful immobilization of a Hoveyda-Grubbs-type catalyst in its pores to study possible pore confinement effects on the MMC selectivity during olefin metathesis reactions. The structure and ordered porosity of large-pore **dHP-TAB** COF with a pore size of 4.8 nm, suitable to accommodate both the bulky molecular catalyst and nm-sized substrates, was ascertained by XRPD analysis and nitrogen sorption experiments. The Ru-catalyst was effectively immobilized by simple silylation on hydroxyl-anchor groups integrated quantitatively in the framework and the retention of the catalyst's structure upon immobilization was confirmed by XANES/EXAFS measurements. A set of four diene substrates for the metathesis reactions, differing in their hydrodynamic radius and polarity, were used to probe the pore confinement effect during the reaction. Our results reveal significant confinement effects, which significantly enhance the macrocyclization over

oligomerization selectivity in the pores as compared to the homogeneous reaction. A clear trend between substrate size and MMC:O selectivity was found and can be attributed to a size-related, slower diffusion of the larger substrates into the pores, thus reducing the efficiency of confinement effects for the larger substrates while enhancing it for the smaller ones. Our results point to the possibility of tailoring the selectivity of metathesis and other size-sensitive catalytic reactions by adjusting the subtle interplay between the size and polarity of both the COF pores and the substrates used for catalysis.

[1]   M. S. Lohse, T. Bein, *Adv. Funct. Mater.* **2018**, *28*, 1705553.
[2]   X. Wang, L. Chen, S. Y. Chong, M. A. Little, Y. Wu, W. H. Zhu, R. Clowes, Y. Yan, M. A. Zwijnenburg, R. S. Sprick, A. I. Cooper, *Nat. Chem.* **2018**, *10*, 1180–1189.
[3]   B. P. Biswal, H. A. Vignolo-González, T. Banerjee, L. Grunenberg, G. Savasci, K. Gottschling, J. Nuss, C. Ochsenfeld, B. V. Lotsch, *J. Am. Chem. Soc.* **2019**, *141*, 11082–11092.
[4]   L. Ascherl, E. W. Evans, M. Hennemann, D. Di Nuzzo, A. G. Hufnagel, M. Beetz, R. H. Friend, T. Clark, T. Bein, F. Auras, *Nat. Commun.* **2018**, *9*, 3802.
[5]   S. Jhulki, J. Kim, I. C. Hwang, G. Haider, J. Park, J. Y. Park, Y. Lee, W. Hwang, A. A. Dar, B. Dhara, S. H. Lee, J. Kim, J. Y. Koo, M. H. Jo, C. C. Hwang, Y. H. Jung, Y. Park, M. Kataria, Y. F. Chen, S. H. Jhi, M. H. Baik, K. Baek, K. Kim, *J. Clean. Prod.* **2020**, *6*, 2035–2045.
[6]   Y. Ge, H. Zhou, Y. Ji, L. Ding, Y. Cheng, R. Wang, S. Yang, Y. Liu, X. Wu, Y. Li, *J. Phys. Chem. C* **2018**, *122*, 27495–27506.
[7]   Y. Zhi, Z. Wang, H. L. Zhang, Q. Zhang, *Small* **2020**, *16*, 2001070.
[8]   S.-Y. Ding, J. Gao, Q. Wang, Y. Zhang, W.-G. Song, C.-Y. Su, W. Wang, *J. Am. Chem. Soc.* **2011**, *133*, 19816–19822.
[9]   H. Xu, J. Gao, D. Jiang, *Nat. Chem.* **2015**, *7*, 905–912.
[10] Q. Sun, Y. Tang, B. Aguila, S. Wang, F. Xiao, P. K. Thallapally, A. M. Al-Enizi, A. Nafady, S. Ma, *Angew. Chemie* **2019**, *131*, 8762–8767.
[11] J. Guo, D. Jiang, *ACS Cent. Sci.* **2020**, *6*, 869–879.
[12] Q. Fang, S. Gu, J. Zheng, Z. Zhuang, S. Qiu, Y. Yan, Q. Fang, S. Gu, J. Zheng, Z. Zhuang, Y. S. Yan, S. Qiu, *Angew. Chem. Int. Ed.* **2014**, *53*, 2878 –2882.
[13] B. Mitschke, M. Turberg, B. List, *Chem* **2020**, *6*, 2515–2532.
[14] C. Heinis, *Nat. Chem. Biol.* **2014**, *10*, 696–698.
[15] S. Monfette, D. E. Fogg, *Chem. Rev.* **2009**, *109*, 3783–3816.
[16] F. Ziegler, J. Teske, I. Elser, M. Dyballa, W. Frey, H. Kraus, N. Hansen, J. Rybka, U. Tallarek, M. R. Buchmeiser, *J. Am. Chem. Soc.* **2019**, *141*, 19014–19022.
[17] J. E. Jee, J. L. Cheong, J. Lim, C. Chen, S. H. Hong, S. S. Lee, *J. Org. Chem.* **2013**, *78*, 3048–3056.
[18] S. T. Emmerling, R. Schuldt, S. Bette, L. Yao, J. Kästner, *ChemRxiv. Cambridge Cambridge Open Engag.* **2021**, DOI 10.33774/chemrxiv-2021-lszg0.

[19]   M. A. Gotthardt, R. Schoch, S. Wolf, M. Bauer, W. Kleist, *Dalt. Trans.* **2015**, *44*, 2052–2056.

[20]   M. Benedikter, J. Musso, M. K. Kesharwani, K. Leonard Sterz, I. Elser, F. Ziegler, F. Fischer, B. Plietker, W. Frey, J. Kastner, M. Winkler, J. van Slageren, M. Nowakowski, M. Bauer, M. R. Buchmeiser, *ACS Catal.* **2020**, *10*, 14810–14823.

[21]   U. Tallarek, J. Hochstrasser, F. Ziegler, X. Huang, C. Kübel, M. R. Buchmeiser, *ChemCatChem* **2021**, *13*, 281–292.

[22]   F. Ziegler, T. Roider, M. Pyschik, C. P. Haas, D. Wang, U. Tallarek, M. R. Buchmeiser, *ChemCatChem* **2021**, *13*, 2234–2241.